24th INTERNATIONAL CONGRESS ON SOUND AND VIBRATION
23–27 July 2017, London

# AN IMPROVED MULTI-HARMONIC BALANCE METHOD FOR NONLINEAR DYNAMIC ANALYSIS FOR JOINT INTERFACE

Wang Dong[1], Feng Jiaquan[2], Hu Jie[3], Wan Qiang[4],

*Institute of Systems Engineering, China Academy of Engineering Physics, Mianyang 621999, P.R.China*

*Email: king_east@sina.cn[1]； fjq@caep.cn[2]; gumu@mail.xjtu.edu.cn[3]; wanzhenyu@126.com[4]*

Mechanics modeling for joints is a challenging problem for the complex multi-scale, multi-physics, nonlinear behaviors of contact interface of the assembled structure. In this paper, the dynamic governing equations of vibration system are conducted with considering the nonlinear stiffness and damping of the joint interface. An improved MHBM (multi-harmonic balance method, MHBM) is then used to analyze the steady-state dynamic response under the periodic loading in time-frequency domain. The proposed method is verified by a comparison with the direct numerical integration solution, and the effect of the nonlinear parameter and periodic exciting frequency is also investigated. The results show that the solutions solved by the proposed harmonic balance method agree well with the direct numerical integration solution. With the increase of the nonlinear parameter, the amplitude of the steady-state response will become smaller, and larger exciting frequency will also induce smaller amplitude of displacement and less area of hysteresis curve.

Key words: joint interface; nonlinear behaviors; steady-state response; MHBM;

## 1. Introduction

The problems of contact and friction modeling for of joint interface are of fundamental importance in structural dynamics [1-3]. The existence of complex multi-scale, multi-physics and nonlinear behaviors of joint interface is mainly response for the complex dynamics of the assembled structures. Modeling for joint interface is critical in the design, control and optimization of mechanical engineering systems [4].

One of practical methods for simulating the nonlinear mechanics of joint interface is employing the deduced-order physics-based models instead of the build-up structure. In this method, developing the physics-based constitutive models for the joint interface is a preparation for the dynamic simulation and prediction. The constitutive models should reproduce the typical nonlinear behaviors of joint interfaces [5, 6]. Several appropriate contact models have been proposed to simulate the stick-slip behaviors [5, 7-12]. Among them are so called stick-slip frictional models, which allow partial slip in contact area of joint interfaces. The Iwan model is commonly used to model the micro-slip behaviors and consists of an array of parallel springs in series with sliders called Jenkins elements [13, 14]. Other frictional models are also used to describe the smooth transition from stick to micro-slip and macro-slip, such as the LuGre bristle friction model, Dahl model, Valanis model [1, 2, 10]. Compared with other constitutive partial slip models, Iwan model can describe the micro-slip of mechanical joint interface better, and the parameters of Iwan model are almost physics-based.

Therefore, the Iwan model has been widely used by many researchers to describe the sliding behaviors, such as Quinn [15], Deshmukh [16], Miller [17].

The aiming of this paper is to develop a modified Iwan model that is capable of describing the nonlinear softening stiffness and hysteresis behaviors of joint interfaces, which is considered to conduct the governing equations of vibration system. The multi-harmonic balance method is used to analyze the steady-state dynamic response under the periodic loading in time-frequency domain. The proposed method is investigated by a comparison with the direct numerical integration solution, and the effect of the nonlinear parameter and periodic frequency is also investigated.

## 2. Contact forces

The nonlinear partial-sliding behaviors of joint interface are modeled using the parallel-series Jenkins elements. Figure 1a) shows the geometry of lab-type joint interface. The up moved part connected to a fixed part with several parallel-series Jenkins elements consistent of spring-slider units, called Iwan model shown in figure 1b). Every Jenkins element has a same stiffness $k_i=k/n$ with a different critical sliding inception force $q_i$, $i=1\ldots n$. Where $n$ is the number of sliders, and $k$ is the total of slipping stiffness. When the tangential load is small, most of sliders keep stick, and the rest sliders will slip for the recycle force of these springs is larger than sliding inception $q_i$, called micro-slip. With the increase of the tangential load, more and more sliders start slipping till all sliders slip, called macro-slip.

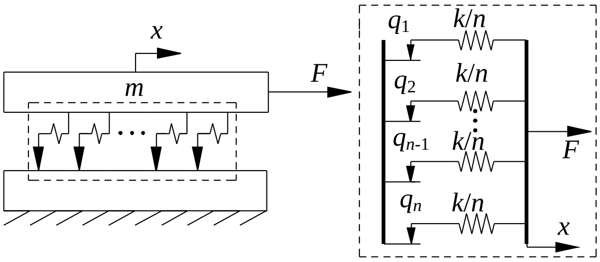


Figure 1 schematic of joint: a) lab-type joint interface, b) Iwan model

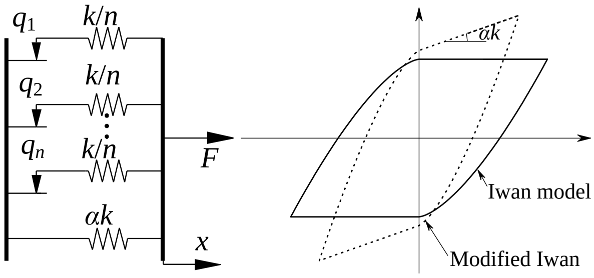


Figure 2 schematic of modified Iwan model: a) modified Iwan model, b) hysteresis curve

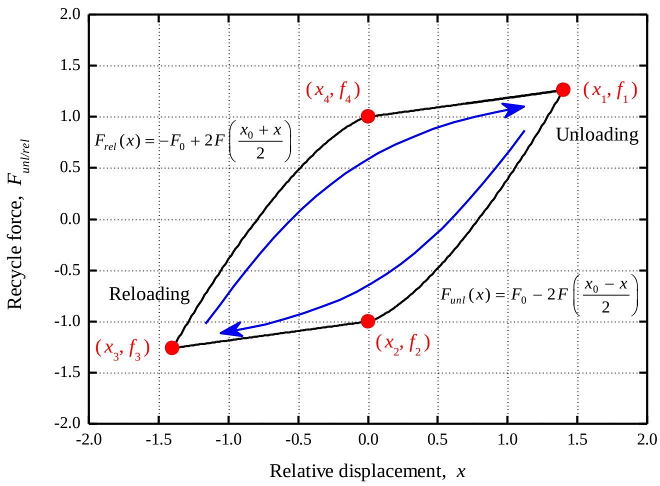


Figure 3 recycle force of joint interface for unloading and reloading process

The Iwan model can well describe the nonlinear stick-slip behaviors of joint interface, but ignore the residual stiffness of the macro-slip. The Iwan model with an additional adjusted spring $k_\alpha=\alpha k$ shown in figure 2a), is applied to describe the residual stiffness of joint interface during the macro-slip.

A uniform distribution of critical sliding force is proposed as

$$\phi(q)=\begin{cases}\dfrac{1}{2f_q} & 0\le q\le 2f_q\\ 0, & else\end{cases} \tag{1}$$

where, $f_q$ is the ultimate slipping force when all of the Jenkins elements slip.

The recycle force of all Jenkins elements can be calculated by

$$F(x)=\int_0^{kx} q\phi(q)dq+kx\int_{kx}^{\infty}\phi(q)dq+\alpha kx \tag{2}$$

Substituting Eq.(1) into Eq.(2) yields

$$F(x)=\begin{cases}(1+\alpha)kx-\dfrac{k^2x^2}{4f_q}, & 0\le x\le 2f_q/k\\ f_q+\ \alpha kx & x\ge 2f_q/k\end{cases} \tag{3}$$

The first part of Eq.(3) is the contribution of Jenkins elements, and the second part is additional adjusted spring's linear recycle force, $\alpha kx$.

In Ref. [6, 9, 18, 19], the parallel-series Iwan model satisfies the Masing hysteresis condition, shown in figure 3. When the joint interface is subjected with oscillatory loading, the recycle force of reloading and unloading process is defined according to the amplitude of recycle force $F_0$ as

$$\begin{cases}F_{rel}(x)=-F_0+2F\left(\dfrac{x_0+x}{2}\right) & \dot{x}\ge 0 \quad reloading\\ F_{unl}(x)=F_0-2F\left(\dfrac{x_0-x}{2}\right) & \dot{x}\le 0 \quad unloading\end{cases} \tag{4}$$

where, $x_0$ denotes the amplitude of relative displacement, related to the amplitude of recycle force $F_0$ and defined as

$$F_0=F(x_0) \tag{5}$$

By substituting Eqs. (1)(2)(5) into Eq.(4), the recycle forces of reloading and unloading process are given by

$$\begin{aligned}F_{unl}(x)&=-\int_0^{k(x_0-x)/2} q\phi(q)dq+kx\int_{kx_0}^{\infty}\phi(q)dq+\alpha kx+\int_{k(x_0-x)/2}^{kx_0}\left(q+kx-kx_0\right)\phi(q)dq\\ F_{rel}(x)&=\int_0^{k(x_0+x)/2} q\phi(q)dq+kx\int_{kx_0}^{\infty}\phi(q)dq+\alpha kx+\int_{k(x_0+x)/2}^{kx_0}\left(kx_0+kx-q\right)\phi(q)dq\end{aligned} \tag{6}$$

## 3. Nonlinear solution methods

The dynamic governing equations of vibration system in time domain are established with the consideration of the local nonlinear behaviors of joint interface, defined as

$$\mathbf{m}\cdot\ddot{\mathbf{x}}+\mathbf{c}\cdot\dot{\mathbf{x}}+\mathbf{k}\cdot\mathbf{x}=\mathbf{f}_{\mathrm{n}}(\dot{\mathbf{x}},\mathbf{x},t)+\mathbf{f}(t) \tag{7}$$

where, **m**、**c**、**k** are separately the mass, linear damping and stiffness matrices. **x** is the response vector of the system degrees of freedom. $\mathbf{f_n}$ is the vector of the nonlinear contact force of joint interface. **f** is the vector of the external force.

The steady-state response in time domain can be reached by the multi-harmonic balance method and defined as

$$\mathbf{x}(\mathrm{t})=\overline{\mathbf{x}}^{(0)}+\Re\left(\sum_{\mathrm{h}=1}^{\mathrm{H}}\overline{\mathbf{x}}^{(\mathrm{h})}\cdot e^{ih\omega t}\right) \tag{8}$$

In this method, the nonlinear contact force and external force are also expressed as a series of harmonic terms.

$$\mathbf{f}_{\mathrm{n}}(\dot{\mathbf{x}},\mathbf{x},t)=\overline{\mathbf{f}}_{\mathrm{n}}^{(0)}+\Re\left(\sum_{\mathrm{h}=1}^{\mathrm{H}}\overline{\mathbf{f}}_{\mathrm{n}}^{(\mathrm{h})}\cdot e^{ih\omega t}\right)$$
$$\mathbf{f}(t)=\overline{\mathbf{f}}^{(0)}+\Re\left(\sum_{\mathrm{h}=1}^{\mathrm{H}}\overline{\mathbf{f}}^{(\mathrm{h})}\cdot e^{ih\omega t}\right) \tag{9}$$

where, H is the number of harmonic terms. $\overline{\mathbf{f}}_{\mathrm{n}}^{(\mathrm{h})}$, $\overline{\mathbf{f}}^{(h)}$ and $\mathbf{x}^{(h)}$ are the Fourier coefficient.

Substituting Eqs.(8)(9) into Eq.(7), and transforming Eq.(7) into frequency domain yields

$$\mathbf{k}\cdot\overline{\mathbf{x}}^{(0)}=\overline{\mathbf{f}}^{(0)}+\overline{\mathbf{f}}_{\mathrm{n}}^{(0)}$$
$$\left[-(h\cdot\omega)^2\cdot\mathbf{m}+i\cdot h\cdot\omega\cdot\mathbf{c}+\mathbf{k}\right]\cdot\overline{\mathbf{x}}^{(h)}=\overline{\mathbf{f}}^{(h)}+\overline{\mathbf{f}}_{\mathrm{n}}^{(h)} \tag{10}$$

where,

$$\overline{\mathbf{x}}^{(h)}=\overline{\mathbf{r}}^{(h)}\cdot\overline{\mathbf{f}}^{(h)}+\overline{\mathbf{r}}^{(h)}\cdot\overline{\mathbf{f}}_{\mathrm{n}}^{(h)}$$
$$\overline{\mathbf{r}}^{(h)}=\left[-(h\cdot\omega)^2\cdot\mathbf{m}+i\cdot h\cdot\omega\cdot\mathbf{c}+\mathbf{k}\right]^{-1} \tag{11}$$

With the results of steady-state response vector in frequency domain, the vector of the velocity can be given by

$$\dot{\overline{\mathbf{x}}}^{(h)}=i\omega\overline{\mathbf{x}}^{(h)}$$
$$\dot{\mathbf{x}}(\mathrm{t})=\dot{\overline{\mathbf{x}}}^{(0)}+\Re\left(\sum_{\mathrm{h}=1}^{\mathrm{H}}\dot{\overline{\mathbf{x}}}^{(\mathrm{h})}\cdot e^{ih\omega t}\right) \tag{12}$$

The interval of the discrete frequency is related to the external oscillatory frequency $f_e$.

$$\omega=n\times2\pi f_e \tag{13}$$

where, $n$ is the discrete number per cycle, $n$>10.

The main steps of the algorithm for getting the steady-state solution **x**(t) is summarized as follows:

① Calculate the steady-state solution **x**(t) of linear system by Eq.(11) without considering the nonlinear contact force $\mathbf{f}_{\mathrm{n}}$ in Eq.(8), and get the velocity by Eq.(13).

② Calculate the nonlinear contact force $\mathbf{f}_{\mathrm{n}}$ in time domain, and transform it to frequency domain by fast Fourier transforming.

③ Calculate the steady-state solution **x**'($t$) by Eq.(11) once more, and also get the velocity by Eq.(13).

④ Calculate the error by comparing the steady-state solution of **x**($t$) and **x**'($t$).

$$\Delta=\left\|\frac{\mathbf{x}(t)-\mathbf{x}'(t)}{\mathbf{x}(t)}\right\| \tag{14}$$

⑤ Remark the error, if Δ<0.01, stop calculating and export the results of step ③, else goto the step ② and recycle the following steps till the error Δ less than 0.01.

# 4. Dynamic governing equation

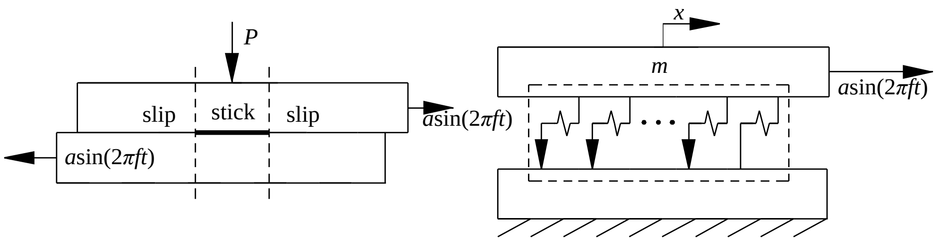


Figure 4 schematic of lap joint: a) contact area of stick and slip, b) simplified jointed structure

When the jointed structure is forced by the normal and oscillatory tangential load synchronously, the contact area can be divided into stick and slip zones shown in figure 4, for the un-uniform distribution of contact stress. The modified Iwan model in Section 2 is applied to describe the nonlinear behaviors of joint interface. Substituting Eqs.(3)(6) into Eq.(7), the dynamic governing equations of lap joint system under oscillatory loading are defined as

$$m\ddot{x}+c\dot{x}+(1-y_s)kx+y_s\times f_{u/l}(\dot{x},x,t)=a\sin(2\pi ft) \tag{15}$$

where, $y_s$ is the proportional coefficient of linear and nonlinear contact force, related to the residual stiffness coefficient $\alpha$, $y_s \in [0,1]$. $f_{u/l}$ denotes the recycle force of unloading and reloading process. $a$ is the amplitude of external exciting force, and $f$ is the frequency.

Transforming Eq.(15) into dimensionless set, the governing equations is multiplied by $(k/mf_q)$.

$$\frac{k}{f_q}\ddot{x}+2\xi\omega\frac{k}{f_q}\dot{x}+(1-y_s)\omega^2\frac{k}{f_q}x+y_s\times\omega^2\frac{f_{u/l}}{f_q}=\frac{k}{mf_q}a\sin(2\pi ft) \tag{16}$$

where, $\omega=(k/m)^{1/2}$, $2\xi\omega=c/m$。

The dimensionless contact force Eq. (3) is given by

$$\bar{f}(y)=\frac{F^{non}}{f_q}=\begin{cases} y-\dfrac{y^2}{4}, & 0\le y\le 2 \\ 1 & y\ge 2\end{cases} \tag{17}$$

where, $y=kx/f_q$.

Substituting Eqs.(4)(17) into Eq.(16) yields

$$\ddot{y}+2\xi\omega\dot{y}+(1-y_s)\omega^2 y+y_s\times\omega^2\bar{f}_{u/l}=\bar{a}\sin(2\pi ft) \tag{18}$$

where, $\bar{a}$ is the dimensionless amplitude of external exciting force, $\bar{a}=ka/mf_q$.

The dimensionless contact force of reloading and unloading process is given by

$$\bar{f}_{u/l}=\begin{cases} f_0^{non}-2\left[\dfrac{y_0-y}{2}-\left(\dfrac{y_0-y}{2}\right)^2\right] & \dot{y}<0 \\ -f_0^{non}+2\left[\dfrac{y+y_0}{2}-\left(\dfrac{y_0+y}{2}\right)^2\right] & \dot{y}>0\end{cases} \tag{19}$$

where, $y_0$ is the maximum dimensionless response. $f_0^{non}$ is the maximum dimensionless recycle force, $f_0^{non}\le 1$, related to $y_0$.

For Eq.(17), the maximum dimensionless contact force is 1. As a result, the recycle force of reloading and unloading process predicted by Eq.(19) is also less than 1. Hence, Eq.(19) is only suitable for micro-slip, and the recycle force of macro-slip is defined as

$$\bar{f}_{u/l}=\begin{cases} -1 & \dot{y}<0 \\ 1 & \dot{y}>0\end{cases} \tag{20}$$

# 5. Results and discussion

## 5.1 Method investigation

In order to validate the proposed multi-harmonic balance method in time-frequency domain, the response of vibration system with the consideration of the nonlinear behaviors is calculated and compared with the direct numerical integration solution. Firstly, the iteration results are shown in figure 5, and the simulated parameters are listed as {$\omega$=1, $\xi$=0.02, $y_s$=0.2, $\bar{a}$=20, $f$=0.5}.

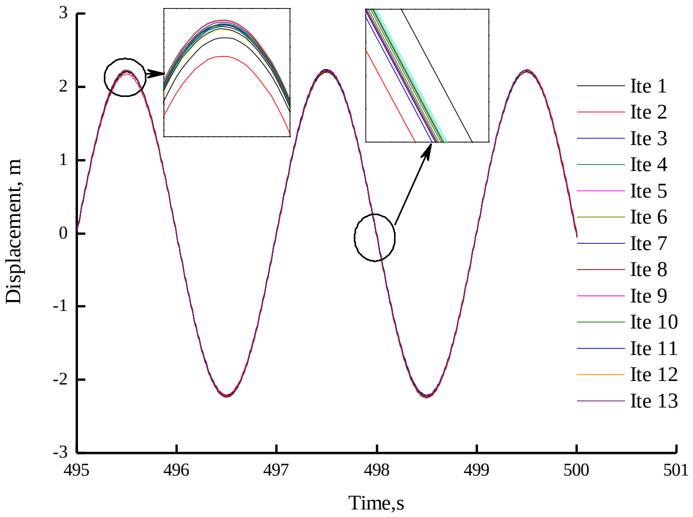


Figure 5 iteration results of proposed MHBM

Figure 5 depicts the steady-state displacement response of 13 iteration cycle. With the increase of iteration cycle, the steady-state response of displacement is convergent till the results satisfy the accuracy. In this paper, the iteration accuracy is 0.001 calculated by Eq.(14). What's more, the accuracy of the proposed method is verified by comparison of displacement, velocity and recycle force with the direct numerical integration solution, shown in figure 6.

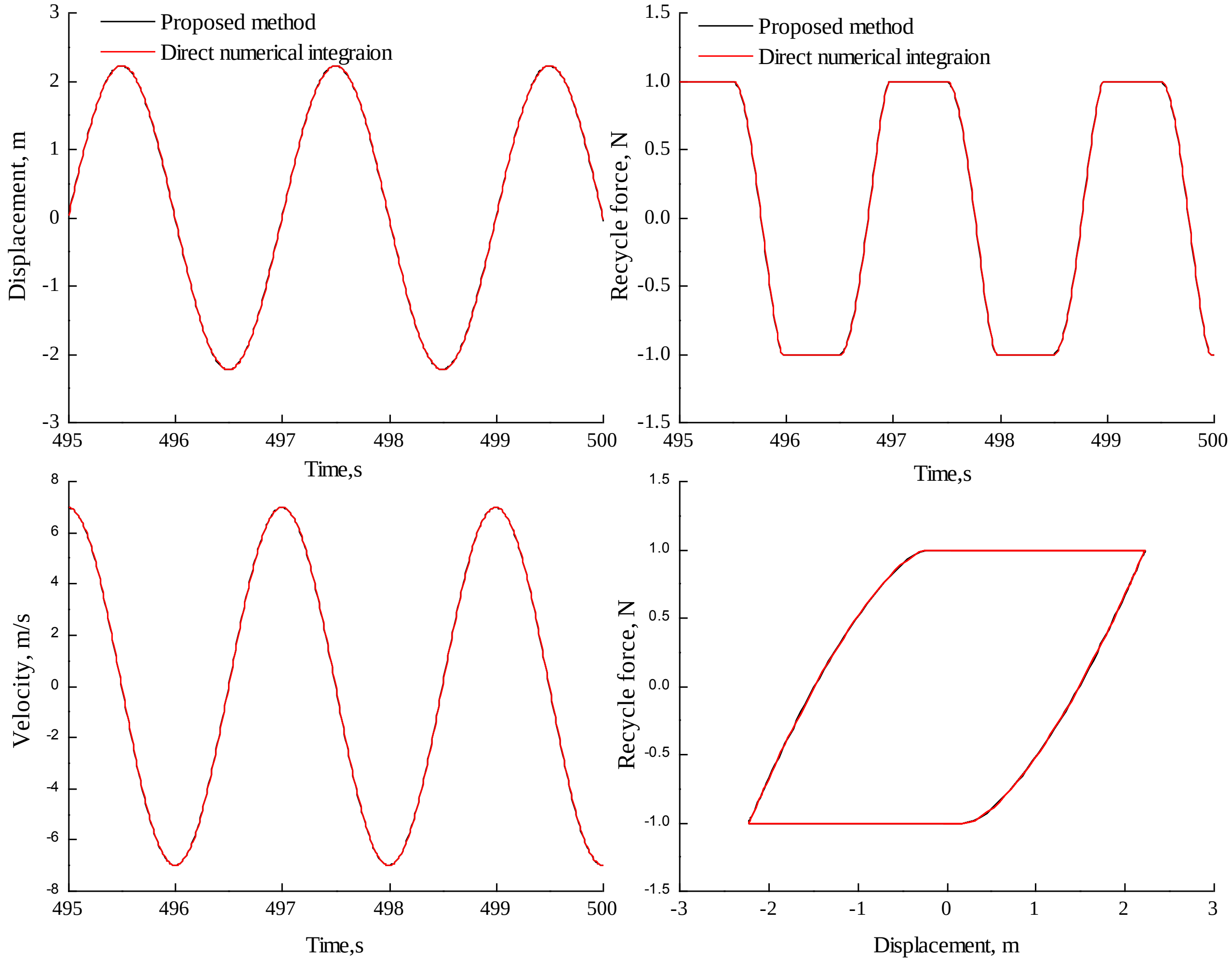


Figure 6 comparison of steady-state response between proposed MHBM and direct numerical integration solution: a) displacement; b) recycle force; c) velocity d) recycle force and displacement

The steady-state response is extracted to investigate the precision by a comparison between the proposed MHBM and direct numerical integration solution shown in figure 6. The results, including displacement response, velocity and recycle force agree well with the direct numerical integration solution. As seen from the relation between the contact force and response shown in figure 4d), with the increase of displacement response, the slop of curve become less and less, inducing a softening stiffness of joint interface.

### 5.2 Parameters investigation

The effect of the nonlinear parameter $y_s$ and exciting frequency on the steady-state response is also investigated. The steady-state response with different nonlinear parameter $y_s$ and the recycle force with different exciting frequency are separately shown in figure 7 and 8.

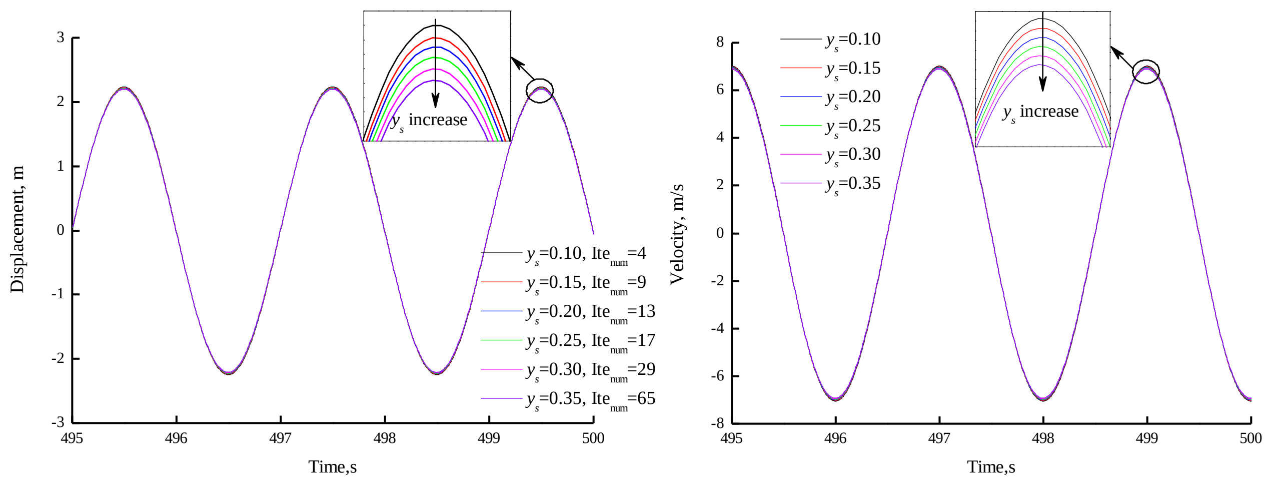


Figure 7 effect of nonlinear parameters on steady-state response: a) displacement, b) velocity

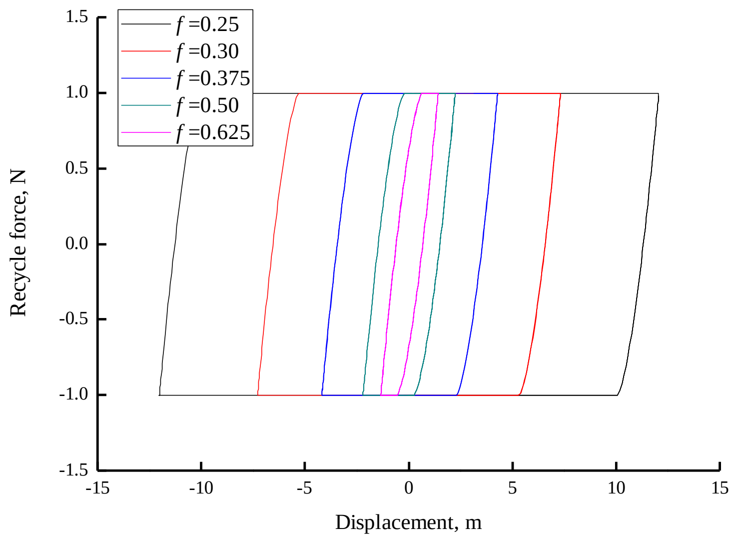


Figure 8 effect of oscillatory frequency on contact force of joint interface

Figure 7 expresses the effect of the nonlinear parameter on steady state displacement and velocity. As seen from figure 7, larger nonlinear parameter $y_s$ will induce smaller displacement amplitude and velocity amplitude, but more cycle number of iteration. The cycle number of iteration at $y_s$=0.1 is 4, while the iteration cycle number is 65 for the case at $y_s$=0.35. Figure 8 depicts the oscillatory frequency on the relation between the contact force and steady-state response. As the oscillatory frequency increases, the amplitude of the steady-state displacement becomes smaller, result in less area of the hysteresis curve and less energy dissipation per cycle.

## 6. Conclusion

In this paper, the modified Iwan model is applied to describe the nonlinear behaviors of joint interface, which is used to conduct the governing equations of vibration system. The multi-harmonic balance method is used to get the steady-state response of jointed structure under oscillatory loading in time frequency domain. The proposed harmonic balance method is verified by a comparison with the numerical integration solution, and the effect of the nonlinear parameter and periodic frequency on the nonlinear behaviors of joint interface is also investigated. The results show that the solutions solved by the proposed harmonic balance method agree well with the direct numerical integration solution. With the increase of the nonlinear parameter, the amplitude of the steady-state displacement and velocity will become smaller. As the periodic frequency increases, the amplitude of displacement will become less, inducing less area of hysteresis curve and less energy dissipation per cycle.

## ACKNOWLEDGMENT

The author thanks the National Natural Science Foundation of China (Grant No. U1530139,11472256), the Presidential Foundation of CAEP (Grant No. YZ2015011) and Focused Science and Technology Development Foundation of CAEP(Grant No. 2014A0203006) for providing the financial support for this project.

## REFERENCES

1 Gaul L., Lenz J., Nonlinear dynamics of structures assembled by bolted joints, *Acta Mechanica*, **125**(1), 169-181, (1997).

2 Gaul L., Nitsche R., The Role of Friction in Mechanical Joints, *Applied Mechanics Reviews*, **54**(2), 93-106, (2001).

3 Segalman D.J., Gregory D.L., Starr M.J., et al., Technical Report SAND2009-4164, Handbook on dynamics of jointed structures, Sandia National Laboratories, Albuquerque, (2009).

4 Ahmadian H., Mottershead J.E., James S., et al., Modelling and updating of large surface-to-surface joints in the AWE-MACE structure, *Mechanical Systems and Signal Processing*, **20**(4), 868-880, (2006).

5 Bograd S., Reuss P., Schmidt A., et al., Modeling the dynamics of mechanical joints, *Mechanical Systems and Signal Processing*, **25**(8), 2801-2826, (2011).

6 Rajaei M., Ahmadian H., Development of generalized Iwan model to simulate frictional contacts with variable normal loads, *Applied Mathematical Modelling*, **38**(15-16), 4006-4018, (2014).

7 Song Y., Hartwigsen C., McFarland D., et al., Simulation of dynamics of beam structures with bolted joints using adjusted Iwan beam elements, *Journal of Sound and Vibration*, **273**(1-2), 249-276, (2004).

8 Segalman D.J., A four-parameter Iwan model for lap-type joints, Transactions of the ASME, *Journal of Applied Mechanics*, **72**(5), 752-760, (2005).

9 Argatov I.I., Butcher E.A., On the Iwan models for lap-type bolted joints, *International Journal of Non-Linear Mechanics*, **46**(2), 347-356, (2011).

10 Abad J., Medel F.J., Franco J.M., Determination of Valanis model parameters in a bolted lap joint: Experimental and numerical analyses of frictional dissipation, *International Journal of Mechanical Sciences*, **89**(1), 289-298, (2014).

11 Mignolet M.P., Song P., Wang X.Q., A stochastic Iwan-type model for joint behavior variability modeling, *Journal of Sound and Vibration*, **349**(4), 289-298, (2015).

12 Li Y., Hao Z., A six-parameter Iwan model and its application, *Mechanical Systems and Signal Processing*, **68-69**, 354-365, (2016).

13 Iwan W.D., A distributed-element model for hysteresis and its steady-state dynamic response, *Journal of Applied Mechanics*, **33**(4), 893-900, (1966).

14 Iwan W.D., On a class of models for the yielding behavior of continuous and composite systems, *Journal of Applied Mechanics*, **34**(3), 612-617, (1967).

15 Quinn D.D., Segalman D.J., Using Series-Series Iwan-Type Models for Understanding Joint Dynamics, *Journal of Applied Mechanics*, **72**(5), 666-673, (2005).

16 Deshmukh D.V., Berger E.J., Begley M.R., et al., Correlation of a discrete friction (Iwan) element and continuum approaches to predict interface sliding behavior, *European Journal of Mechanics - A/Solids*, **26**(2), 212-224, (2007).

17 Miller J.D., Quinn D., A two-sided interface model for dissipation in structural systems with frictional joints, *Journal of Sound and Vibration*, **321**(1-2), 201-219, (2009).

18 Segalman D.J., Starr M.J., Technical Report SAND2004-4321, Relationships among certain joint constitutive models, Sandia National Laboratories, Albuquerque, (2004).

19 Segalman D.J., Starr M.J., Inversion of Masing models via continuous Iwan systems, *International Journal of Non-Linear Mechanics*, **43**(1), 74-80, (2008).